Progress In Electromagnetics Research C, Vol. 76, 207–219, 2017

A Single Layer S/X-Band Series-Fed Shared Aperture Antenna for SAR Applications

Venkata K. Kothapudi and Vijay Kumar*

Abstract—This paper presents our research work on designing a dual-band dual-polarized (DBDP) series-fed S/X-band shared aperture antenna (SAA) for synthetic aperture radar (SAR) applications. The proposed SAA DBDP X-band antenna is designed with the concept of series-fed 4-group 2×2 planar arrays with high impedance microstrip line feeding in both vertical and horizontal polarizations. By etching out the inner edge elements from 2×2 X-band subarrays in all the four-groups, the S-band element could be accommodated. The design evolution stages have been presented. The S-band (3.2 GHz) is best suited for volumetric soil moisture estimation using SAR and X-band (9.3 GHz) best suited for surveillance SAR applications and grain size estimation. To verify the antenna design concept, a prototype is fabricated and measured with both S-parameters and radiation characteristics including gain measurements. The antenna with reflection coefficient $|S_{11}| < -10$ dB has an impedance bandwidth 3.12–3.42 GHz (9.3% BW) in S-band and 9.2–9.36 GHz (1.72% BW) in X-band. The measured isolation lS21l between two different bands in the same polarization is better than 25 dB, and the isolation between two different bands in two orthogonal ports is better than 30 dB. Measured gain of the antenna at S-band is better than 8.5 dBi at V-port and H-port, and X-band is better than 11 dBi at either port. Measured side-lobe level (SLL) at S-band is better than -17 dB at either port, and X-Band is better than -20 dB at either port. The overall size of the S/X-DBDP SAA is $100 \times 100 \times 1.6\,\text{mm}^3$. Measured results of the S/X-DBDP SAA show good agreement with the finite integration technique (FIT) based computer simulation technology (CST) microwave studio.

1. INTRODUCTION

Dual-band dual-polarized antennas can offer lot of advantages for synthetic aperture radar. The dual-band operations of the antenna can provide frequency diversity to the radar. Dual-polarization operation can provide polarization diversity, thus enhance the information content by providing orthogonal polarization scattering data. Since the 1970s, the remote sensing synthetic aperture radar (SAR) systems have been rapidly evolving. The SIR-C/X SAR mounted on the American Space Shuttle Endeavour firstly completed the high resolution 3D imaging all over the globe in Feb. 2000 [1]. It consists of three individual dual-polarized subarrays operating at L-, C-, and X-bands, respectively. This resulted in large and bulky structure weighing over 3000 kg. The multiband dual-polarized array receives more target information than the single-band single-polarization counterpart, and thus enhances the detection and identification of targets range and azimuth by means of radio waves. The common bands for space borne SARs are the L, S, C, and X-bands. To minimize the volume and weight of the SAR antenna, a shared aperture configuration for dual- or multi-bands are required, which will share the sub-systems behind the arrays [2–15]. A shared aperture antenna SAA in L- and C-bands is proposed by Pokuls et al. in [2] to fill the gap of shared aperture antenna technology using multilayer, which uses slots in the L-band and interlaced with microstrip patches operating in the C-band. Pozar and

Received 1 July 2017, Accepted 8 August 2017, Scheduled 19 August 2017
* Corresponding author: Vijay Kumar (vijaykumar@vit.ac.in).
The authors are with the School of Electronics Engineering, VIT University, Vellore, Tamilnadu 632014, India

Targonski [3] presented an L/X-DBDP SAA for space borne SAR using aperture coupled patches with good cross-polarization performance, which had multilayer configuration. This design yields 3.2% and 15.5% bandwidths at L- and X-bands, respectively. In 2001, Karmakar et al. [4] described a photonics bandgap (PBG) assisted SAA for very small aperture terminals (VSAT) applications operating at S/X 3.8 and 6.28 GHz using a 3-layer configuration. Differently sized radiating elements were presented in [5], to increase the total bandwidth and reduce the mutual coupling between the radiators interleaved on a common aperture. Zhong et al. [6] proposed a triple-band dual-polarization (TBDP) L/S/X-bands with frequency ratio of $1 : 2.8 : 8$, which had a 5-layer configuration. A DBDP SAA L/S-band using stacked patch with unsymmetrical crossed slots was implemented to improve the isolation and cross-polarization performance with multilayer configuration. The bandwidth improvement in both L/X-bands can be achieved using stacked patches, proposed in [8]. Another SAA technique with 8-layers using a square ring shaped radiating element at L-band and square shaped patch at S-band on different substrate layers was presented by Sharma et al. [9]. Zhou et al. [10] proposed a wideband, low profile SAA operating at two extreme bands P/Ku with dual linear polarizations and single linear polarization at Ku- and P-bands, respectively. A novel sandwiched stacked patch structure for C-band and fully perforated patch to improve the lower band bandwidth is proposed in [11]. Zhou et al. [12] provided differential feeding methods, and corporate binary feed networks were used to enhance the isolation between polarizations and good radiation pattern characteristics, respectively. A linear/circularly polarized SAA using parabolic reflector with prime focus configuration at S-band and Cassegrain feed configuration at Ka-band was proposed in [13]. A concept of Fabry-Perot resonant cavity as a metasurface to reduce the complexity of the SAR antenna was presented by Qin et al. in 2016 [14]. A shared aperture helical array antenna set at L- and S-bands and realized for navigation satellite systems with concentric phase center located at the two bands is proposed in [15]. So far, all the previous studies have multilayer configuration with microstrip technology for low profile, parabolic reflector antenna and helical antenna for dual band-and triple-band SAA system. There is no single-layer configuration which will cater DBDP SAA technology. The objective of this paper is to fill the gap. Series-fed and parallel fed networks are two possible arrangements for feeding these types of arrays presented in [16]. Compared with the parallel fed arrangements, series-fed networks have the benefits of simplicity and compactness which can be translated into low-loss feeding structures proposed by Pozar and Schaubert [17]. Rocca and Morabito in 2015 [20] proposed a new approach for array synthesis for a reconfigurable planar array radiating sum and difference patterns, which allows maximizing the radiation performance including field slope and directivity of both beam patterns over assigned directions. Sharing part of the excitation amplitudes has been implemented between the two radiation modalities for reducing the complexity of the beam forming networks.

Obtaining dual linear polarization dual-band SAA with single-layer PCB is a big challenge. The basic objective of this article is to design and develop a SAA technology in single-layer PCB with frequency and polarization diversity. Instead of using two separate dedicated antennas for S- and X-bands, shared aperture antenna technology is used here. A systematic design for dual linear polarizations at S- and X-bands with high port isolation has been discussed. Realized prototypes have been experimentally investigated. The proposed design should find potential applications in SAR with frequency diversity and polarization diversity.

In this paper, a low cost and low profile SAA antenna design prototype for S/X-band SAR applications is presented. The proposed antenna designs operate at S/X frequency bands covering 3.2/9.3 GHz. The substrate thickness of 0.787 mm with 1 oz copper cladding makes the prototypes flexible. The photo film of the exported DXF file is used for fabrication. The antenna is fabricated using UV exposure machine HHT-12 (common exposure machine) according to the dimensions provided in Section 2. The detailed design analysis and results for prototype are discussed in Sections 2 and 3, respectively. The prototypes are tested using VNA for S-parameters measurements and anechoic chamber for radiation pattern measurement. The effects of SMA connectors and Sucoform microwave cables used in the measurement setup are not considered in the simulations. Finally, the work is concluded in Section 4.

2. ANTENNA STRUCTURE AND DESIGN

In this work, an RT/Duroid-5880 (made by Rogers) copper cladding substrate with 31 mil (0.787 mm) height, 1 oz, i.e., 0.035 mm thick copper with a relative permittivity $\varepsilon_r = 2.2$ and loss tangent $\tan\delta = 0.0009$, is chosen as the antenna material [18]. All the metal components in the reported antenna design are taken to be copper with its known material parameters $\varepsilon r = 1$, $ur = 1$ and bulk conductivity $\sigma = 5.8 \times 10^7$ s/m. After fabrication of the antenna, we had gone through gold plating over the patch and ground copper layer of 1-micron thickness for better conductivity. Later, antenna mounting plate with brass material of 0.8 mm thickness is mechanically fabricated which is used to mount the antenna PCB using M2 (M-Metric Standard) Stainless Steel screws. Now the height of the antenna becomes 1.6 mm (electrical dimensions: $0.07\lambda_g$), and previously it was 0.8 mm ($0.035\lambda_g$) without brass plate. The overall size of the S/X-DBDP SAA is $100 \times 100 \times 1.6\,\text{mm}^3$ (or) $3.1 \times 3.1 \times 0.0496\lambda_0^3$ with respect to the velocity of propagation in air (or) $3.92 \times 3.92 \times 0.0627\lambda_g^3$ with respect to the velocity of propagation in substrate material, which corresponds to the X-band center frequency 9.3 GHz. All simulations are performed using CST Microwave Studio 2016 [19], industry standard simulation software based on FIT-Finite Integration Technique that is equivalent to FDTD-Finite Difference Time Domain simulation approach.

2.1. S-Band Element and X-Band Subarray Design

The configuration of the S-band single patch is depicted in Figure 1 with dual linear polarizations (both vertical and horizontal polarizations) with all the antenna physical parameters. The patch is excited using 50 Ω direct coupled microstrip line feeding for both vertical and horizontal polarizations. The width of the matching transformer section of the direct coupled feed line is MWS = 2.46 (2.54 = 48.5 Ω) to obtain the impedance of 50 Ω. After that, a quarter wave impedance transformer with quarter wave transformer length for S-band (QLS) and quarter wave transformer width for S-band (QWS) is used to improve the impedance characteristics of the proposed antenna. The final optimized parameters of the proposed S-band element are given in Table 2. In Figure 2, the $|S_{11}| < -10$ dB plots show the best case with QLS = 20 mm ($\lambda_g/4 = 17.62$ mm; guided wavelength (λ_g) = 70.5 mm at 3.2 GHz), and QWS is 0.8 mm (which is approximately 93.5 Ω). The frequency response of the S-band element is shown in Figure 2, which indicates that the antenna resonates at 3.2 GHz at both vertical and horizontal ports. The impedance bandwidth covers from 3.12 to 3.42 GHz (9.3%) for $|S_{11}| < -10$ dB and the isolation $S_{21}| < -20$ dB in the entire band. The polarization mechanism for V-port and H-port are depicted in Figure 6(a) as surface current distribution.

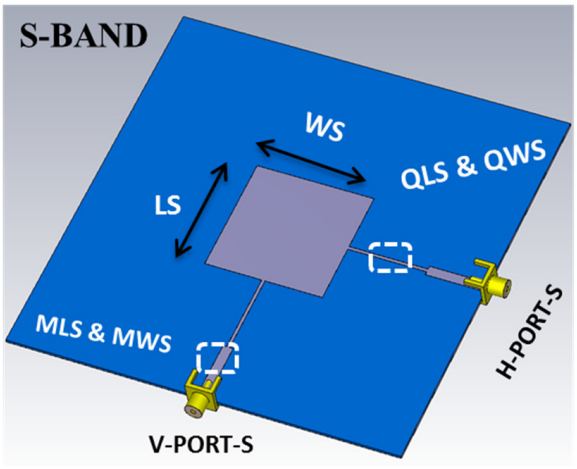

Figure 1. Geometry of S-band dual port element.

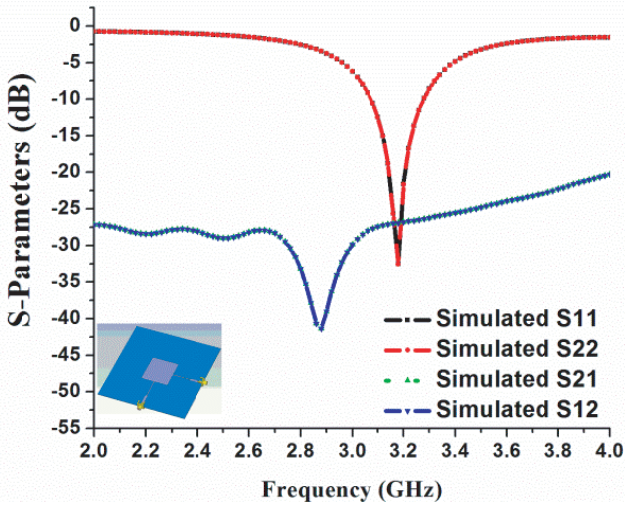

Figure 2. Simulated S-parameters of S-band element.

Table 1. S-band different parameters of the proposed antenna unit. (Value of the parameters of the proposed antenna).

Parameter	LS	WS	QLS	QWS	MLS	MWS
Value (mm)	30	30	20	0.8	15	2.54
Value (λ_0)	0.32	0.32	0.213	0.0085	0.16	0.027
Value (λ_g)	0.4377	0.4377	0.291	0.0116	0.218	0.037
mm: millimeter λ_0: Free space wavelength with respect to the velocity of propagation in air center frequency (3.2 GHz) (0.09375 meters) λ_g: Guided wavelength with respect to the velocity of propagation in substrate material (RT-Duroid-5880) (0.06853 meters)						

Table 2. X-band different parameters of the proposed antenna unit. (Value of the parameters of the proposed antenna).

Parameter	LX	WX	QLX	QWX	MLX	MWX	SFL	SFW
Value (mm)	10.2	10.2	5.0	0.76	7.0	2.34	22	0.8
Value (λ_0)	0.316	0.316	0.155	0.0235	0.217	0.0725	0.682	0.024
Value (λ_g)	0.432	0.432	0.212	0.0322	0.296	0.099	0.933	0.0339
mm: millimeter λ_0: Free space wavelength with respect to the velocity of propagation in air center frequency (9.3 GHz) (0.03225 meters) λ_g: Guided wavelength with respect to the velocity of propagation in substrate material (RT-Duroid-5880) (0.02357 meters)								

Figure 3 shows the geometry and configuration of the proposed X-band unit cell subarray. The antenna is fed through a 50 Ω matching transformer in vertical and horizontal polarizations. The width of the matching transformer section of the direct coupled feed line is MWX = 2.34 (= 51 Ω) to obtain the impedance of 50 Ω. Next, a quarter wave impedance transformer QLX and QWX is used to improve the impedance characteristics of the proposed antenna. The $|S_{11}| < -10$ dB plots shows good impedance

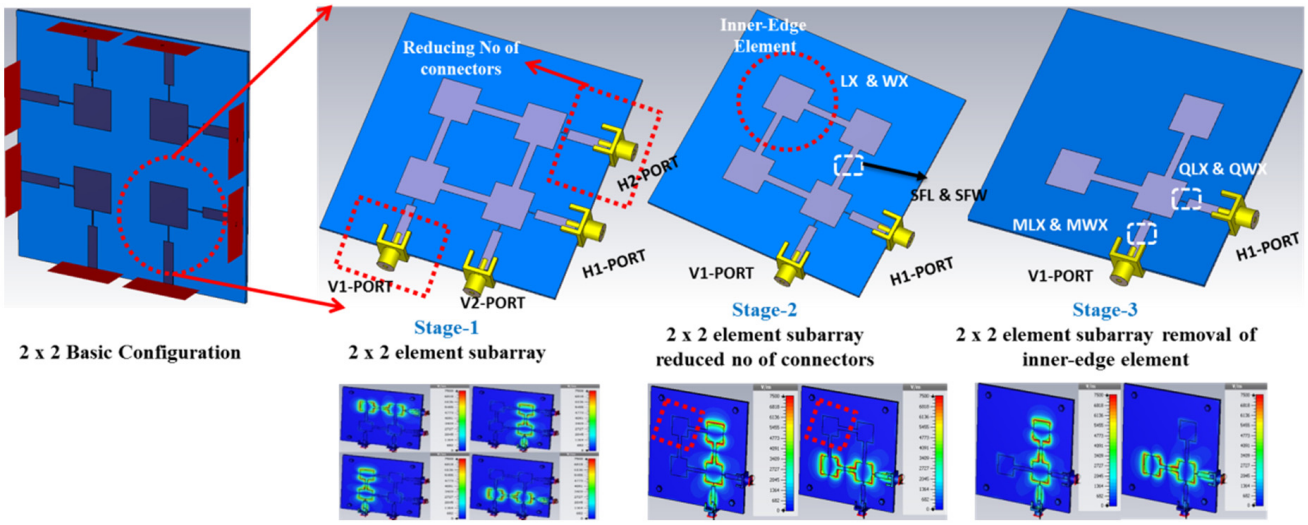

Figure 3. Evolution stages of proposed X-band 2 × 2 subarray with Surface current distribution.

matching at QLX = 5 mm ($\lambda_g/4$ = 6 mm; guided wavelength (λ_g) = 24 mm at 9.3 GHz), and QWS is 0.76 mm (which is approximately 95.5 Ω). The final optimized parameters of the proposed X-band element are given in Table 2. Further, the single group of 2 × 2 series-fed planar arrays with V-ports and H-ports as unit-cell for X-band design as stage-1, reduced number of controls or connectors as stage-2 and removal of inner edge element (to accommodate the S-band element in S/X DBDP SAA) to create 1 × 2 linear array in both X- and Y-directions with surface current distributions are shown in Figure 3. The final optimized parameters of the proposed X-band subarray are given in Table 2. The frequency response of the X-band element and 1 × 2 linear array are depicted in Figures 4(a) and (b), which indicate that the antenna resonates at 9.3 GHz at both vertical and horizontal polarizations. The impedance bandwidth covers from 9.2 to 9.36 GHz (1.72%) for $|S_{11}| < -10$ dB and the isolation $|S_{21}| < -30$ dB in the entire band.

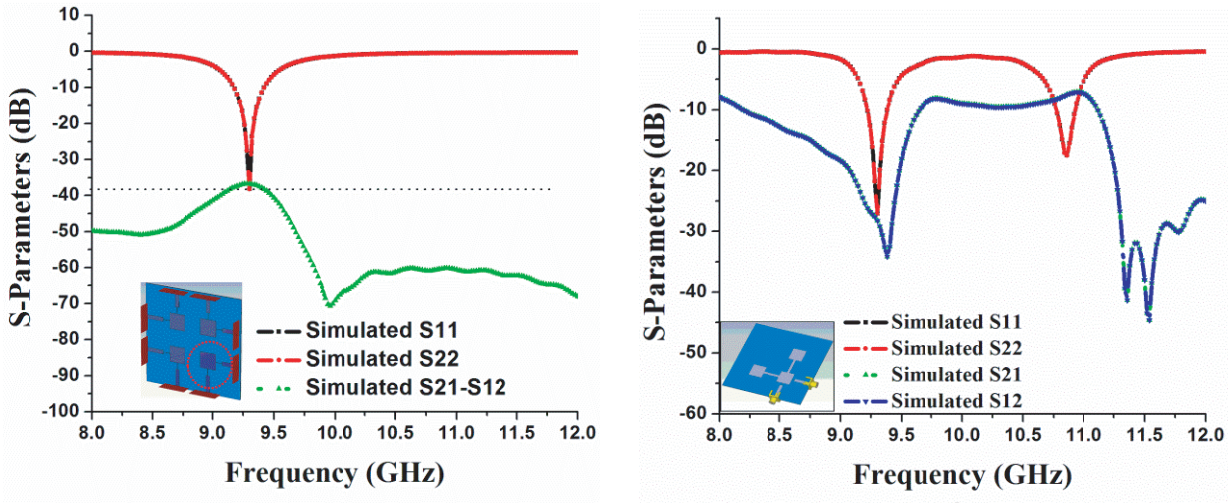

Figure 4. (a) Simulated S-parameters of X-band basic configuration. (b) Simulated S-parameters of X-band 1 × 2 subarray configuration.

3. EMBEDDING S/X DBDP SHARED APERTURE ANTENNA

The geometry configurations of the proposed S/X-band SAA with evolution stages are illustrated in Figure 5. The array consists of 4 groups of identical series-fed 2 × 2 planar antenna array with element group mirroring in both vertical and horizontal planes, and the element group is implemented with vertical (V1 & V2) and horizontal (H1 & H2) ports for dual polarizations shown as stage-1, reduced number of controls or connectors shown as stage-2, inner edge elements etched out for all 4 groups as stage-3 (now the 2 × 2 planar array becomes 1 × 2 linear array in X- and Y-directions), and finally, the S-band element is accommodated in stage-4, which are represented with clear notations in Figure 5 and surface current distribution for all ports at 9.3 GHz in Figure 6(b). The series-fed X-band array has a feed width (SFW) which is optimized to 0.8 mm. The typical inter-element spacing employed in X-band array is in the range of 0.7λ, which corresponds to center frequency 9.3 GHz (approximately one-guided wavelength), which is SFL = 22 mm in this SAA X-band linear array. Optimal spacing is used to save the number of antenna elements for a narrow beamwidth and directivity. The element distance is restricted by scan requirement factors. In X-band 1 × 2 linear array, the element distance for square distribution can be decided in X- and Y-directions simply by Equations (1) & (2).

$$d_x = \frac{\lambda_V}{1 + \sin\theta_x} \tag{1}$$

$$d_y = \frac{\lambda_H}{1 + \sin\theta_y} \tag{2}$$

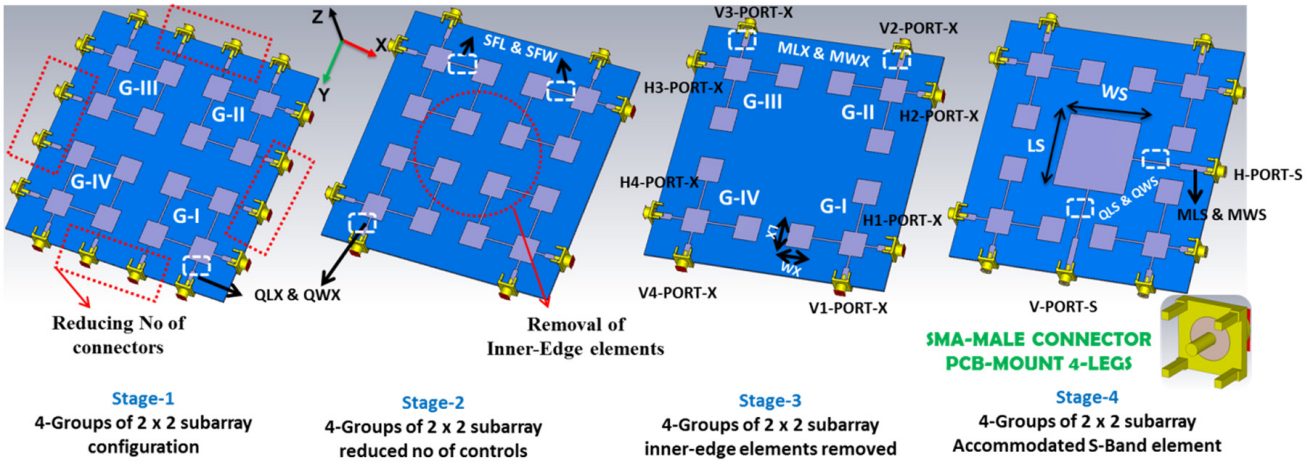

Figure 5. S/X-DBDP SAA Geometry of evolution stages.

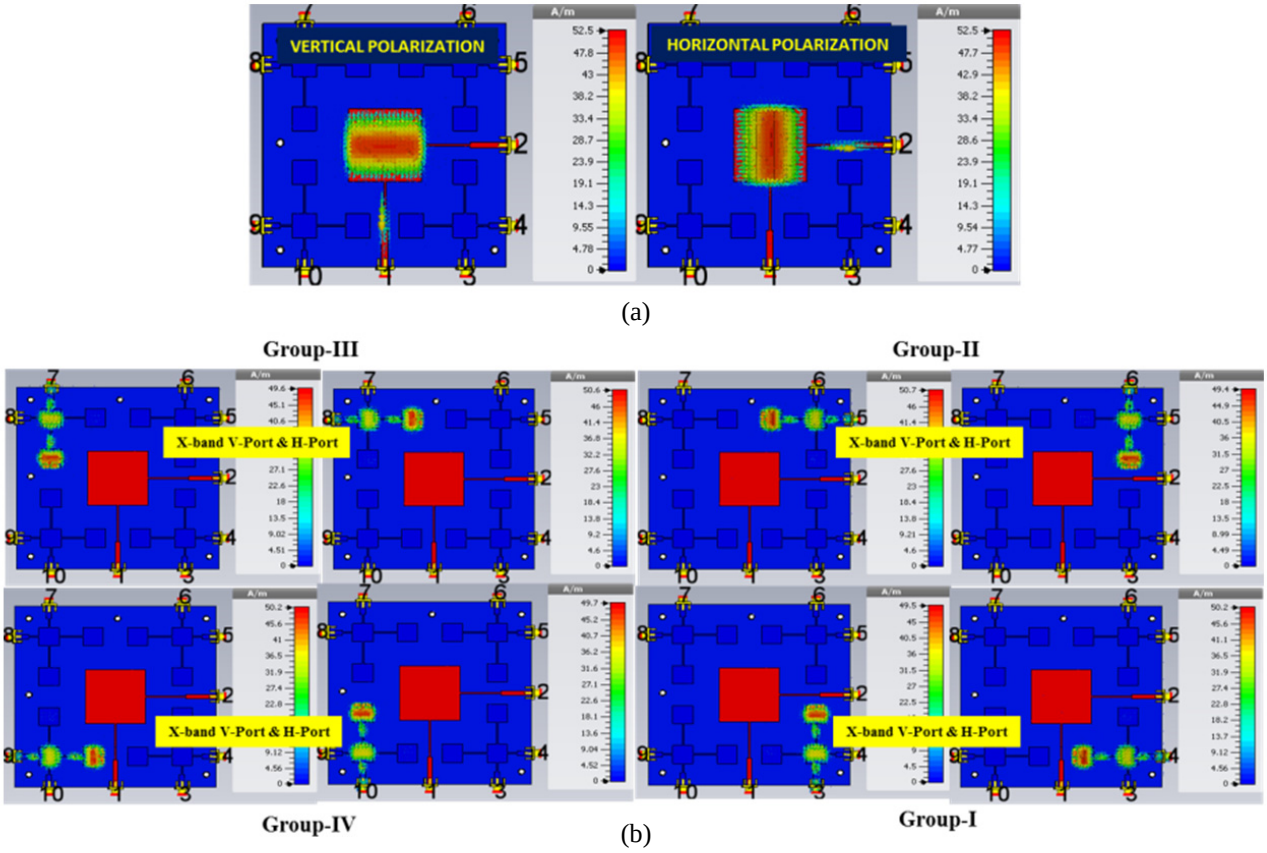

Figure 6. Surface current distribution of S/X-DBDP SAA for all ports. (a) S-band. (b) X-band.

where λ_V and λ_H are the vertical and horizontal free space wavelengths of 9.3 GHz. d_x and d_y are the distances between the elements in X- and Y-directions. θ is the maximum scan angle of 25°.

Simulation is carried out by full-wave electromagnetic simulation software, and the final structure parameters including brass plate dimensions of complete S/X DBDP shared aperture antenna are given in Tables 1, 2, and 3.

Table 3. Different parameters of the proposed substrate material and brass plate.

Mechanical mounting plate (Brass material) M2-Stainless Steel (SS) Fixing Screws							
Parameter	BPL	BPW	BPH				
Value (mm)	100	100	0.8				
Substrate Material (RT/Duroid-5880) ($L \times W \times H$)							
Parameter	L	W	H	Parameter	L	W	H
Value mm	100	100	0.787	Value mm	100	100	0.787
Value (λ_0) @3.2 GHz	1.06	1.06	0.0053	Value (λ_0) @9.3 GHz	3.1	3.1	0.0248
Value (λ_g) @3.2 GHz	1.349	1.349	0.0106	Value (λ_g) @9.3 GHz	3.92	3.92	0.0308
mm: millimeter; B: Brass; L: Length; W: Width; H: Height.							

4. SIMULATED AND EXPERIMENTAL RESULTS AND ANALYSIS

The S/X DBDP shared-aperture array prototype, with central frequencies of 3.2 GHz and 9.3 GHz for S- and X-bands, respectively, is fabricated and measured to validate the design. As shown in Figure 7, the prototype array is incorporated with S/X-bands. The simulated and measured results are given only one group for X-band due to brevity. The S-parameters and radiation patterns are measured using Agilent N9918A Field fox microwave vector network analyzer, and the radiation patterns and gain measurements are measured in an anechoic chamber (supplier: Haining ocean import and export Co. Ltd) of 6 m × 4 m × 3 m ($L \times W \times H$) with Agilent PNA series network analyzer N5230C (10 MHz to 40 GHz). The measurement setups for both S-parameters and radiation pattern are shown in Figures 8(a)–(f).

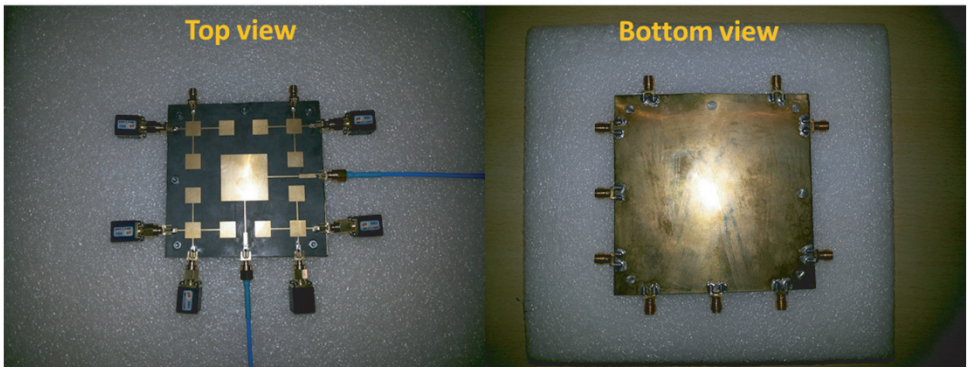

Figure 7. Fabricated prototype top and bottom view photograph of S/X-DBDP SAA.

The measured reflection coefficient S_{11} of the proposed S/X-band SAA is presented in Figure 9. The results show measured reflection coefficient bandwidth from 3.12–3.42 GHz (9.3%) at S-band for both vertical and horizontal polarizations and 9.2–9.36 GHz (1.75%) at X-band for both vertical and horizontal polarizations with a resonant frequency of 3.2 GHz and 9.3 GHz, respectively. The results agree well with simulated and measured antenna parameters. Isolation higher than 25 in both S- and X-bands is obtained. Figure 10 gives the simulated and measured isolation results between S/X-bands. In addition, Figure 11 shows the measured isolation between two different bands in the same polarization which is better than 25 dB, and isolation between two different bands in two orthogonal ports is better than 30 dB. The notations of VV ports refers to S-band vertical port and X-band vertical port; VH ports refers to S-band vertical port and X-band horizontal port; HV ports refers to S-band horizontal port and X-band vertical port; HH ports refers to S-band horizontal port and X-band horizontal port.

Radiation patterns of the antenna system are measured at either port at both S- and X-bands as shown in measurement setup in anechoic chamber and are displayed in Figures 6(a) & (b). Measured

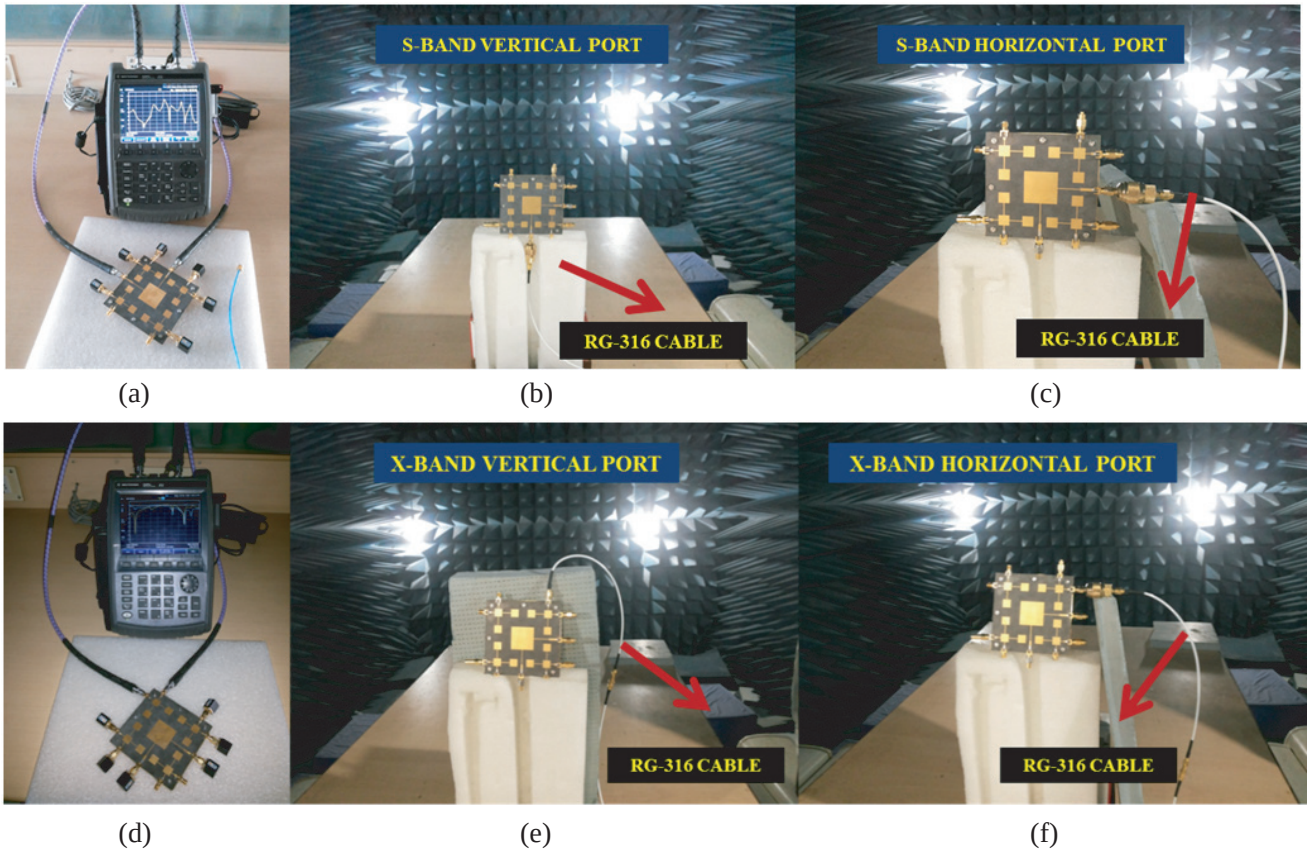

Figure 8. S-band measurement setup: (a) S-parameters with VNA, (b) radiation pattern measurement with vertical port, (c) radiation pattern measurement with horizontal port. X-band measurement setup: (d) S-parameters with VNA, (e) radiation pattern measurement with vertical port, (f) radiation pattern measurement with horizontal port.

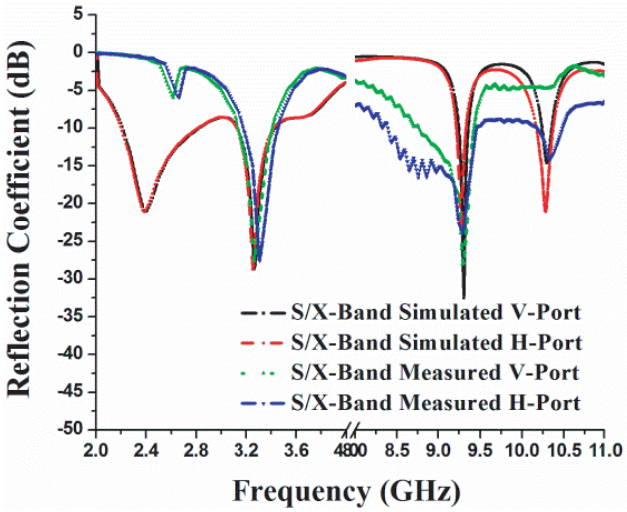

Figure 9. Simulated and measured reflection coefficient of S/X-DBDP SAA.

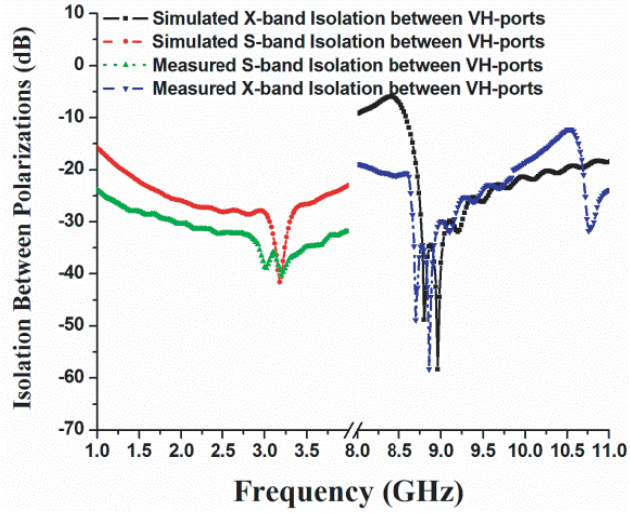

Figure 10. Simulated and measured isolation between bands of the S/X-DBDP SAA.

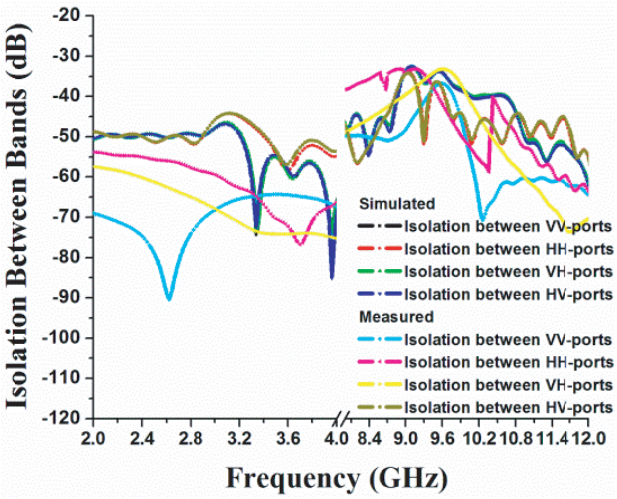

Figure 11. Simulated and measured isolation between bands of the S/X-DBDP SAA.

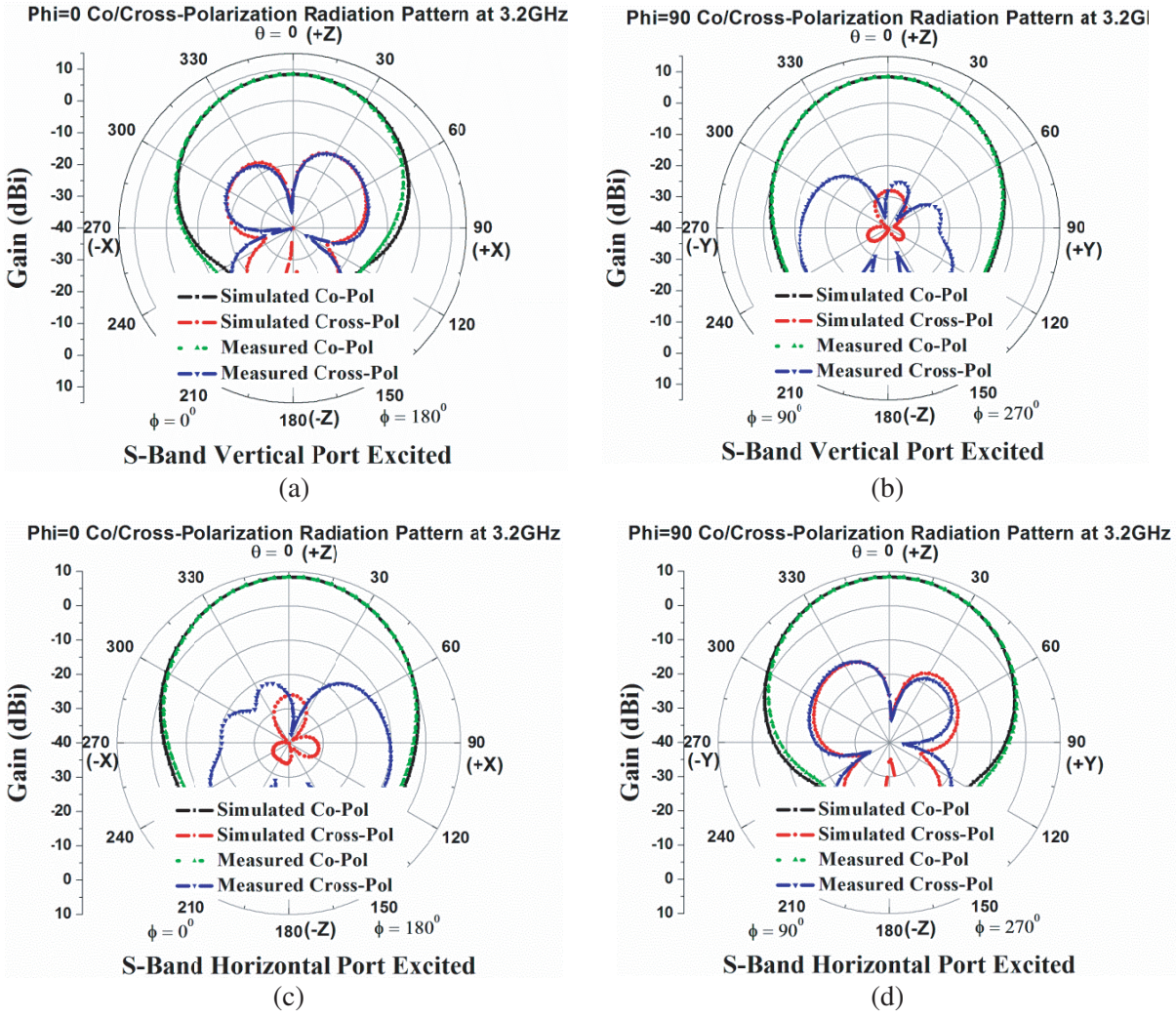

Figure 12. (a) V-Port excited Phi = 0°-plane @3.2 GHz. (b) V-Port excited Phi = 90°-plane @3.2 GHz. (c) H-Port excited Phi = 0°-plane @3.2 GHz. (d) H-Port excited Phi = 90°-plane @3.2 GHz.

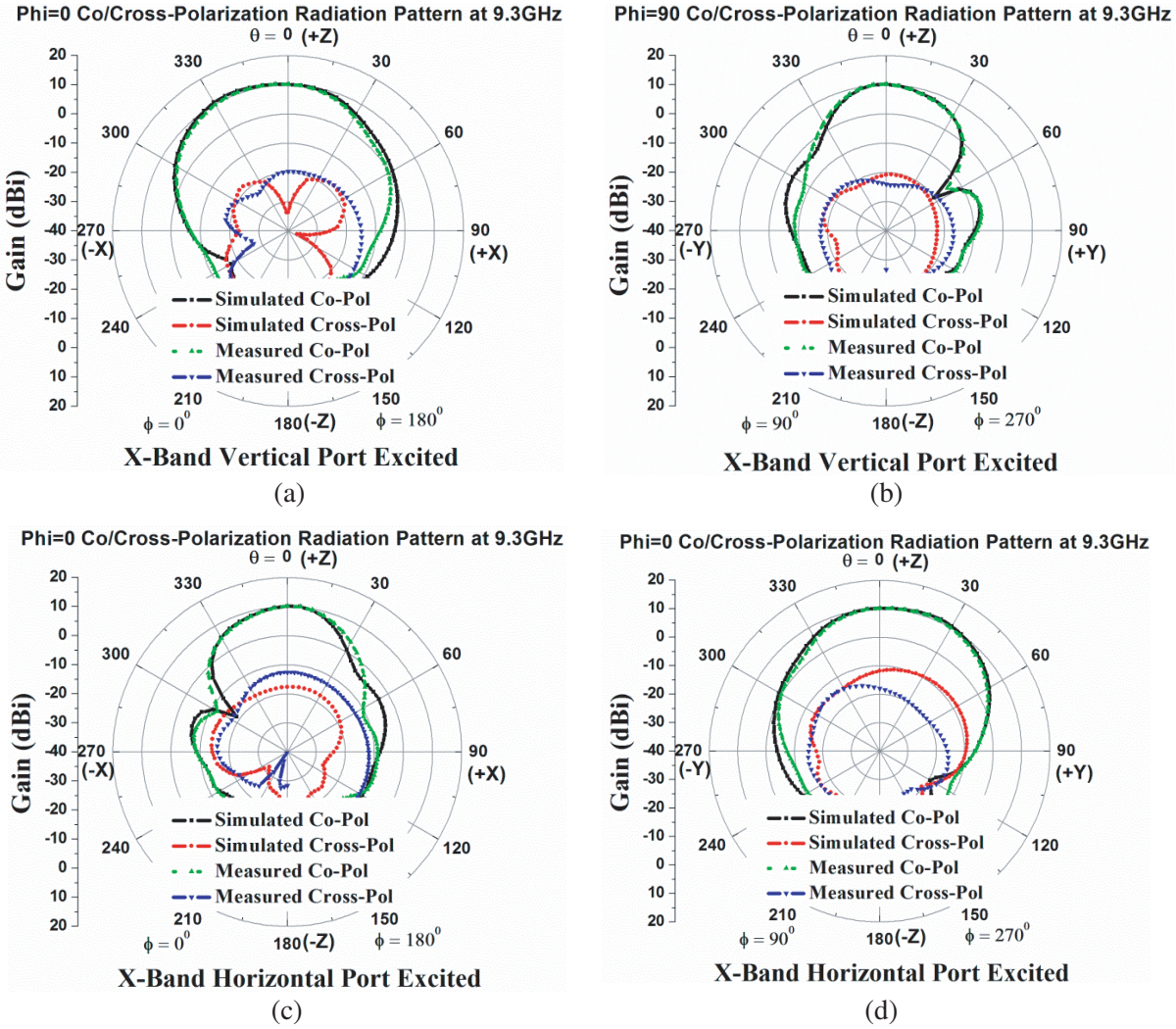

Figure 13. (a) V-Port excited Phi = 0°-plane @9.3 GHz. (b) V-Port excited Phi = 90°-plane @9.3 GHz. (c) H-Port excited Phi = 0°-plane @9.3 GHz. (d) H-Port excited Phi = 90°-plane @9.3 GHz.

radiation patterns of the S-band antenna at port-1 and port-2 (V-port and H-port) at 3.2 GHz are two orthogonal planes (Phi = 0° & Phi = 90°) and are shown in Figures 12(a)–(d). Measured radiation patterns of the X-band antenna (group-1) at port-1 and port-2 (V-port and H-port) at 9.3 GHz are two orthogonal planes (Phi = 0° & Phi = 90°) and are shown in Figures 13(a)–(d). Good agreement between the simulated and measured results is obtained with directional characteristics. It can be found that the peak radiation happens in the broadside direction at these two frequencies. The cross polarization level at 3.2 GHz in the Phi = 0° & Phi = 90°-planes in both vertical and horizontal polarizations is below −20 dB. The cross polarization level at 9.3 GHz in the Phi = 0° & Phi = 90° planes in both vertical and horizontal polarizations is below −15 dB. The measured SLL is less than −17.9 dB in both Phi = 0° & Phi = 90°-planes at 3.2 GHz in H-polarization. Meanwhile, the cross-polarization level less than −25 dB in the two principal planes is achieved. Similar results are obtained in V-polarization in the S-band. At 9.3 GHz, the SLL remains below −22.4 and −13.5 dB in the Phi = 0° & Phi = 90°-planes in the two polarizations.

The measured gains are calculated using gain-transfer method, and standard gain horn (SGH) is used as a reference antenna during the measurement. The simulated and the measured realized gains of this antenna are shown in Figure 14. The measured peak gain occurs at 3.2 GHz in V-polarization and H-polarization, reaching 8.43 and 8.42 dBi, respectively, corresponding to efficiencies of 89.41% and 88.6%.

In the X-band, both the peak gains in dual-polarizations occur at 9.3 GHz, which are around 10.6 dBi and 10.56 dBi in the two polarizations and corresponding to efficiencies of 88.8% and 88.76%. The front-to-back ratios (FTBR) over both the S- and X-bands are presented in Figure 15. The FTBR values are from 11 to 15 dB at 3.2 GHz and 23.5 to 25 dB at X-band (9.3 GHz), respectively. The 3 dB beamwidths (HPBW) over the S- and X-bands are depicted in Figure 16. The antenna performance characteristics such as side lobe level (SLL), front-to-back ratio (FTBR), gain, 3 dB beamwidth (HPBW), efficiency and cross-polarization (X-pol) level are calculated and summarized in Table 4.

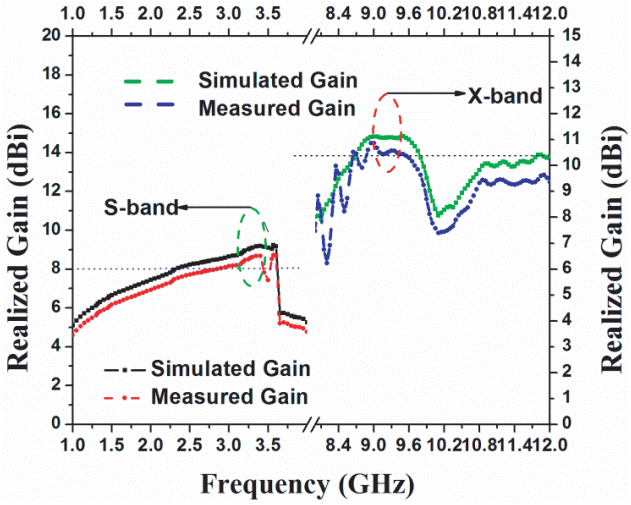

Figure 14. Simulated and measured realized gain of the S/X-DBDP SAA.

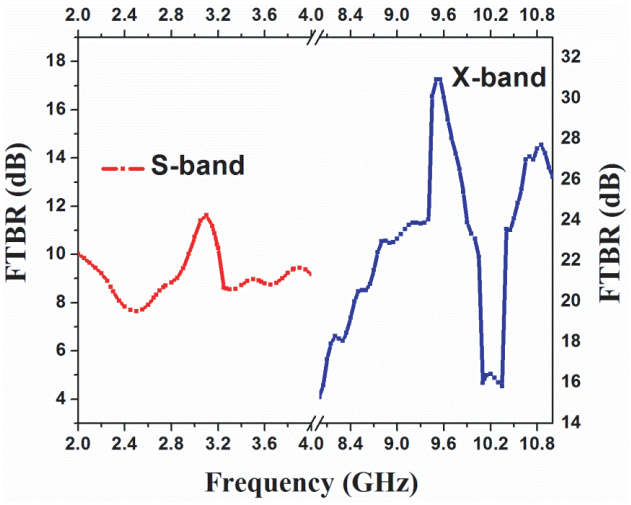

Figure 15. Front-to-back ratio over frequency S/X DBDP SAA.

Table 4. Measured radiation parameters of the S/X-band Shared aperture antenna (SAA).

Parameter		S-Band (3.2 GHz)		X-Band (9.3 GHz) Group-I	
		V-Port	H-Port	V-Port	H-Port
Band width		3.12–3.42	3.12–3.42	9.2–9.36	9.2–9.36
Gain		8.43	8.42	10.6	10.56
Radiation efficiency		88.8	88.76	89.41	88.6
E-Plane	SLL (dB)	−17.9	−17.9	−22.4	−13.5
	HPBW (deg)	73.2	65.4	69.3	40.3
	Cross-pol (dB)	−28.1	−26.1	−33	−20
	FTBR (dB)	10.26	15	23.83	25
H-Plane	SLL (dB)	−17.9	−17.9	−13.5	−22.4
	HPBW (deg)	65.4	73.2	40.3	69.3
	Cross-pol (dB)	−28.1	−26.1	−19	−24
	FTBR (dB)	11	15	23.83	25
Aperture area (Ap)		$100 \times 100\,\text{mm}^2$			
Effective area (Ae)		$65 \times 30\,\text{mm}^2$		$44.4 \times 44.4\,\text{mm}^2$	
Aperture efficiency (ea)		19.5%		19.71%	
Note: For X-band one group is 19.71% for all 4-groups 19.71 × 4, i.e., 78.84% For S-band the utilization effective area is 19.5% Efficient utilization of S/X-DBDP SAA is 98.34%					

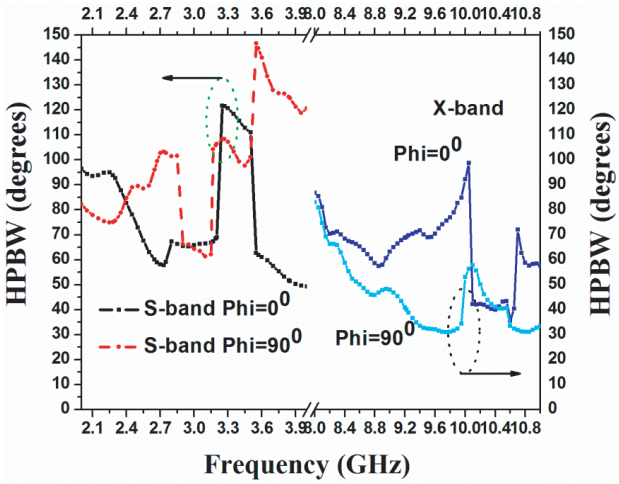

Figure 16. 3 dB beam width over frequency S/X DBDP SAA.

5. CONCLUSION

A shared aperture DBDP series-fed antenna operating at both S- and X-bands for SAR applications is presented in this paper. Single square-shaped element with microstrip line feeding is used as S-band antenna, and four-groups of 2×2 subarrays are used as X-band elements. Inner edge elements in X-band 2×2 subarray are etched off, to make it 1×2 linear arrays, to accommodate the S-band dual-polarized square patch antenna. A prototype of this antenna is fabricated and experimentally measured. The measured results show that the SAA is in good agreement with simulated ones in comparison with both S-parameters and radiation characteristics including gain measurements. The S/X-DBDP SAA has narrow FBW of 9.3% at 3.2 GHz and 1.72% at 9.3 GHz, respectively. The total size of the S/X-DBDP shared aperture antenna is compact and occupies an area of $100 \times 100 \times 1.6\,\text{mm}^3$. The SAA is best suited for large size array antenna for the SAR applications. The proposed SAA has many advantages, such as single-layer structure, easy fabrication, low production cost and good isolation between the bands and between the polarizations. The proposed S/X-DBDP SAA is also suitable for synthesis of the array. In future, the authors intend to make a synthesis of the array for radar and reconfigurable field applications with larger array configuration.

ACKNOWLEDGMENT

The work has been done at Microwave division, School of Electronics Engineering (SENSE), VIT University, Vellore, and Tamilnadu, India. DST provided financial support for this work with grant reference number SB/DGH-82/2013. All the assistance provided by the department and university administration to carry out this work is highly appreciated. The authors express their thanks to reviewers of this manuscript.

REFERENCES

1. Jordan, R. L., B. L. Huneycutt, and M. Werner, "The SIR-C/X-SAR synthetic aperture radar system," *IEEE Trans. Geosci. Remote Sens.*, Vol. 33, 829–839, 1995.
2. Pokuls, R., J. Uher, and D. M. Pozar, "Dual-frequency and dual-polarization microstrip antennas for SAR applications," *IEEE Trans. Antennas Propag.*, Vol. 46, 1289–1296, 1998.
3. Pozar, D. M. and S. D. Targonski, "A shared-aperture dual-band dual polarized microstrip array," *IEEE Trans. Antennas Propag.*, Vol. 49, 150–157, 2001.

4. Karmakar, N. C., Md. N. Mollah, S. K. Padhi, and J. S. Fu, "PBG-assisted shared-aperture dual-band aperture-coupled patch antenna for satellite communication," *Microw. Opt. Technol. Lett.*, Vol. 16, 289–292, 2005.
5. Coman, C. I., I. E. Lager, and L. P. Ligthart, "The design of shared aperture antenna consisting of differently sized elements," *IEEE Trans. Antennas Propag.*, Vol. 54, 376–383, 2006.
6. Zhong, S.-S., Z. Sun, L.-B. Kong, C. Gao, W. Wang, and M.-P. Jin, "Tri-band dual polarization shared-aperture microstrip array for SAR applications," *IEEE Trans. Antennas Propag.*, Vol. 60, 4157–4165, 2012.
7. Kong, L.-B., S.-S. Zhong, and Z. Sun, "Broadband microstrip element design of a DBDP shared-aperture SAR array," *Microw. Opt. Technol. Lett.*, Vol. 54, 133–136, 2012.
8. Zhou, S. G., T. H. Chio, and J. Lu, "A shared-aperture dual-wideband dual-polarized stacked microstrip array," *Microw. Opt. Technol. Lett.*, Vol. 54, 486–491, 2012.
9. Sharma, D. K., S. Kulshrestha, S. B. Chakrabarty, and R. Jyoti, "Shared aperture dual band dual polarization microstrip patch antenna," *Microw. Opt. Technol. Lett.*, Vol. 55, 917–922, 2013.
10. Zhou, S. G., P. K. Tan, and T. H. Chio, "A wideband, low profile P and Ku-band shared aperture antenna with high isolation and low cross-polarization," *IET Microwaves Antennas Propag.*, Vol. 7, 223–229, 2013.
11. Sun, Z., K. P. Esselle, S.-S. Zhong, and Y. J. Guo, "Shared-aperture dual-band dual-polarization array using sandwiched stacked patch," *Progress In Electromagnetics Research C*, Vol. 52, 183–195, 2014.
12. Zhou, S.-G., J.-J. Yang, and T.-H. Chio, "Design of L/X-band shared aperture antenna array for SAR application," *Microw. Opt. Technol. Lett.*, Vol. 57, 2197–2204, 2015.
13. Chakrabarti, S., "Development of shared aperture dual configuration antenna for S/Ka-band communication," *Microw. Opt. Technol. Lett.*, Vol. 58, 139–145, 2015.
14. Qin, F., S. Gao, Q. Luo, C.-X. Mao, C. Gu, G. Wei, J. Xu, J. Li, C. Wu, K. Zheng, and S. Zheng, "A simple low-cost shared-aperture dual-band dual-polarized high-gain antenna for synthetic aperture radars," *IEEE Trans. Antennas Propag.*, Vol. 64, 2914–2922, 2016.
15. Kumar, S. S., H. C. Sanandiya, R. Jyoti, A. K. Singhal, D. K. Jangid, and R. C. Gupta, "A shared aperture helical-array antenna set at L and S bands for navigation satellite systems," *IEEE Antennas Propag. Mag.*, Vol. 42, 144–151, 2017.
16. James, J. and P. Hall, *Handbook of Microstrip Antennas*, *Ser. IEEE Electromagnetic Waves Series*, Peter Peregrinus Ltd., London, United Kingdom, 1989.
17. Pozar, D. and D. Schaubert, "Comparison of three series fed microstrip array geometries," *Proc. IEEE Antennas Propag. Soc. Int. Symp.*, 728–731, IEEE, 2002.
18. Rogers Corporation, Available at: www.rogerscorp.com.
19. Computer simulation technology version (2016), Wellesley Hills, MA. Available at: www.cst.com.
20. Rocca, P. and A. F. Morabito, "Optimal synthesis of reconfigurable planar arrays with simplified architectures for monopulse radar applications," *IEEE Trans. Antennas Propag.*, Vol. 63, 1048–1058, 2015.